Saturation Wind Effects on the Dynamics of a Modified Leslie-Gower Predator-Prey Model: Stability and Ecological Implications

Fengde Chen, Jiaxing Ye, Guangwen He, and Yuting Huang

***Abstract*—This paper proposes a modified Leslie-Gower predator-prey model incorporating saturation wind effects to explore the nonlinear impact of wind speed on ecosystem dynamics. By introducing a saturation function $\phi(\omega) = 1+\frac{\omega}{k+\omega}$, we analyze the system's stability, persistence, and bifurcation behavior. Key findings include:**

1) **Critical Wind Speed (ω_c): A critical wind speed ω_c is identified, beyond which the system transitions from a coexistence state to prey extinction, highlighting wind speed's role in ecosystem stability.**
2) **Saturation Effect: At low wind speeds, predation rate increases linearly with wind speed but saturates at high wind speeds, reflecting organisms' adaptive strategies to extreme conditions. This saturation effect balances predation pressure and prey survival.**
3) **Global Stability and Persistence: The positive equilibrium E^* is globally asymptotically stable when $r > \alpha\phi(\omega)c$, ensuring predator-prey coexistence. The system is also shown to be persistent under this condition.**
4) **Transcritical Bifurcation: The system undergoes a transcritical bifurcation at ω_c, where the positive equilibrium E^* collides with the prey-free equilibrium $E_1(0, c)$, leading to a state transition.**

Numerical simulations validate the theoretical results, demonstrating how wind speed influences ecosystem dynamics. This study provides a new perspective on the interplay between climatic factors and biological interactions, with implications for ecological conservation and pest control.

***Index Terms*—Leslie-Gower, predator-prey model, stability, saturation wind effects**

I. Introduction

In nature, predator-prey relationships are one of the most fundamental interspecies interactions. As such, they have been a long-standing focus of research for biomathematicians, as seen in references [1]-[31] and the cited literature. Recently, scholars have begun to pay attention to the impact of wind on the dynamical behavior of predator-prey systems [17]-[22]. Among them, Jawad, Sultan, and Winter [17], based on observations from [16] that reed warblers' nests exposed to wind may lead to an increased detection rate by aerial predators, proposed the following predator-prey system with wind effects:

Manuscript received February 16, 2025; revised April 26, 2025. This work is supported by the Natural Science Foundation of Fujian Province(2024J01273).

F. D. Chen is a professor of College of Mathematics and Statistics, Fuzhou University, Fuzhou, CHINA (e-mail: fdchen@fzu.edu.cn).

J. X. Ye is a postgraduate student of College of Mathematics and Statistics, Fuzhou University, Fuzhou, CHINA (e-mail: 2246519132@qq.com).

G. W. He is a postgraduate student of College of Mathematics and Statistics, Fuzhou University, Fuzhou, CHINA (e-mail: 594047408@qq.com).

Y. T. Huang is a postgraduate student of College of Mathematics and Statistics, Fuzhou University, Fuzhou, CHINA (e-mail: 1104943637@qq.com).

$$\begin{aligned} \frac{du}{dt} &= ru\Big(1-\frac{u}{K}\Big) - \frac{\alpha uv}{\phi(\omega)} - equ, \\ \frac{dv}{dt} &= sv\Big(1-\frac{v}{\phi(\omega)+\beta u+c}\Big) - \gamma v, \end{aligned} \tag{1}$$

where $\phi(\omega)$ represents the wind effect. The authors thoroughly investigated the dynamic behavior of this model. However, numerical simulations in [17] showed that as wind speed increases, the population densities of both predators and prey increase. This is counterintuitive, as higher wind speeds would make reed warblers' nests more easily detectable, implying that the warblers are more likely to be captured, and thus their population density should decrease. Therefore, the results of [17] do not align with the ecological background described above. Recently, Huang, Chen, Zhu, and Li[18] argued that model (1) does not reflect reality and proposed a more reasonable model:

$$\begin{aligned} \frac{du}{dt} &= ru\Big(1-\frac{u}{K}\Big) - \alpha\phi(\omega)uv - equ, \\ \frac{dv}{dt} &= sv\Big(1-\frac{v}{\beta\phi(\omega)u+c}\Big), \end{aligned} \tag{2}$$

where $\phi(\omega) = 1 + \omega$. Their research demonstrated that as wind speed increases, the prey population indeed decreases, while the predator population increases, which aligns with the observations in [16].

If we consider more natural scenarios of population survival, model (1) can be further improved. In fact, under the influence of wind, both prey and predator populations adopt certain strategies:

- **Prey Behavior and Survival**:
  - *Predator Avoidance*: Wind affects the prey's sensory and mobility capabilities. At low wind speeds, prey can more clearly use visual, auditory, and other senses to detect approaching predators and take timely evasive actions, so the impact of wind on predator avoidance is minimal. As wind speed increases, the sound of the wind may mask the predator's noises, and wind may also interfere with the prey's vision (e.g., by raising dust), making it harder for the prey to detect predators, thus increasing the risk of predation. However, when wind speed reaches a certain level, strong winds may also severely limit the predator's mobility, making it difficult for flying predators to maintain stable flight and accurately capture prey. Additionally, prey may find sheltered areas or adopt specific wind-resistant behaviors to avoid predation, so the impact of wind

on predation risk no longer increases significantly, showing a saturation effect. For example, hares on grasslands can detect approaching hawks well in light winds; in strong winds, although it becomes harder to detect hawks, the difficulty of hunting for hawks also increases, and hares may hide in burrows or other sheltered areas, causing the impact of wind on predation risk to saturate.

– *Foraging Behavior*: Wind also affects the foraging activities of prey. At low wind speeds, prey can relatively easily search for food within a specific range. As wind speed increases, it may scatter or bury some plant-based food resources, increasing the difficulty of foraging. However, when wind speed reaches saturation, prey may change their foraging strategies, such as seeking food sources less affected by strong winds (e.g., underground roots) or reducing foraging activities and waiting for the wind to subside. Thus, the impact of wind on prey foraging also saturates at high wind speeds. For example, some insects can typically forage for nectar on flowers in light winds, but in strong winds, the nectar may be blown away or the flowers damaged, making foraging difficult. However, when the wind becomes extremely strong, insects may hide on the undersides of leaves or other sheltered spots, no longer being further affected by the wind.

- **Predator Behavior and Hunting Efficiency**:

  – *Prey Localization*: Predators rely on various sensory cues to locate prey, and wind can interfere with these cues. Predators can use low wind speeds to track prey through smell, hearing, and other senses. As wind speed increases, it may disperse the prey's scent and mask the sounds made by the prey, reducing the predator's ability to locate prey. However, when wind speed exceeds a saturation point, predators may abandon sensory cues severely affected by strong winds and adopt other relatively stable hunting strategies, such as using vision to search for prey in open areas less affected by wind or waiting for prey in specific terrains (e.g., leeward slopes). Thus, wind interference on predator localization no longer increases significantly at high wind speeds, showing a saturation effect. For example, foxes hunting voles can track vole burrows by scent in light winds, but the scent is dispersed in strong winds. However, in powerful winds, foxes may choose to wait in open areas where voles frequently appear, using vision to observe vole movements, so the impact of wind on their hunting localization no longer increases with further increases in wind speed.

  – *Hunting Actions*: For flying or highly mobile predators, wind speed directly affects their hunting actions. Low wind speeds help predators maintain stable flight or movement for hunting. As wind speed increases, predators need to expend more energy to counteract the wind, reducing the flexibility and accuracy of their hunting actions. When wind speed reaches a saturation point, predators' physical capabilities and behavioral strategies limit the extent to which their hunting efficiency decreases with further increases in wind speed. For example, raptors can easily soar and dive to hunt in low winds, but in strong winds, flying becomes difficult. However, in robust winds, raptors may adjust their flight altitude and speed to find relatively stable air currents, so the impact of wind on their hunting actions no longer increases indefinitely with wind speed.

Based on the above observations and analysis, a predator-prey model considering the saturation effect of wind may better reflect the actual ecological background. Therefore, we propose the following model:

$$\begin{aligned} \frac{du}{dt} &= ru\left(1-\frac{u}{K}\right)-\alpha\phi(\omega)uv \stackrel{\text{def}}{=} uF_1(u,v), \\ \frac{dv}{dt} &= sv\left(1-\frac{v}{\beta\phi(\omega)u+c}\right) \stackrel{\text{def}}{=} vF_2(u,v), \end{aligned} \tag{3}$$

where

$$\begin{aligned} F_1(u,v) &= r\left(1-\frac{u}{K}\right)-\alpha\phi(\omega)v, \\ F_2(u,v) &= s\left(1-\frac{v}{\beta\phi(\omega)u+c}\right), \end{aligned} \tag{4}$$

and

- $\phi(\omega)=1+\frac{\omega}{k+\omega}$ is the saturation function, ω is the wind speed, and k is the saturation constant, representing the wind speed at which the effect saturates. When $\omega\to 0$, $\phi(\omega)\to 1$; when $\omega\to\infty$, $\phi(\omega)\to 2$. This indicates that the impact of wind speed increases with wind speed at low wind speeds but saturates at high wind speeds. The choice of saturation function is motivated by its ability to capture both linear response at low wind speeds and adaptive saturation at high speeds. Comparatively, classical linear models (e.g., $\phi(\omega)=1+\omega$) in [17] fail to reflect behavioral adaptations observed in field studies [16].
- r is the intrinsic growth rate of the prey population, K is the environmental carrying capacity of the prey population, α is the predation efficiency coefficient, and αw is the number of prey consumed by a single predator in the absence of wind.
- s is the intrinsic growth rate of the predator population, and c represents other food sources.

In the above model (3), we make the following assumptions:

- **Prey Equation**:
  – The growth of the prey population is limited by the environmental carrying capacity K.
  – The predation rate $\alpha\phi(\omega)$ is influenced by wind speed but saturates as wind speed increases.
- **Predator Equation**:
  – The growth of the predator population is limited by the prey density, with a carrying capacity of $\beta\phi(\omega)u+c$.
  – Wind speed affects the predator's carrying capacity through $\phi(\omega)$, but the effect saturates as wind speed increases.

This paper aims to thoroughly investigate the dynamical behavior of system (3) and provide a definitive answer to how wind effects influence the system's dynamics. The paper is organized as follows: In the next section, we will explore the positivity and boundedness of the solutions to the system (3); in Section 3, we will analyze the existence of equilibrium points; In Section 4, we investigate the local stability of the equilibrium points; in Section 5, we will discuss the extinction property of the system; in Section 6, we will discuss the global stability of the equilibrium points; in Section 7, we will examine the persistence property of the system; in Section 8, we will investigate the influence of wind effect; in Section 9, we state the discoveries of the paper; in Section 10, we will present numerical simulations to validate our theoretical findings; and finally, we will summarize the impact of wind effects on the dynamical behavior of system (3) and highlight our discoveries.

II. Positivity and Boundedness of Solutions to System (3)

The following result is obtained regarding the positivity of solutions to system (3).

Theorem 2.1 *The positive quadrant $R_2^+ = \{(u,v)|u > 0, v > 0\}$ is an invariant set for system (3).*

Proof. From (3), for all $t \in [0, +\infty)$, we have:

$$\begin{aligned} u(t) &= u(0)\exp\left\{\int_0^t F_1(u,v)dt\right\} \\ &> 0, \end{aligned}$$

$$\begin{aligned} v(t) &= v(0)\exp\left\{\int_0^t F_2(u,v)dt\right\} \\ &> 0. \end{aligned}$$

This completes the proof of Theorem 2.1.

Theorem 2.2. *For system (3), the solutions $u(t)$ and $v(t)$ with the initial conditions $u(0) > 0$ and $v(0) > 0$ are uniformly bounded.*

Proof. From the first equation of system (3), we have:

$$\frac{du}{dt} \le ru(1 - \frac{u}{K}),$$

An application of Lemma 2.3 in [25] to the preceding inequality leads to:

$$\limsup_{t\to+\infty} u(t) \le K. \tag{5}$$

Hence, for any sufficiently small positive constant $\varepsilon > 0$, there exists a time $T_1 > 0$ such that for all $t \ge T_1$, the following inequality holds:

$$u(t) < K + \varepsilon. \tag{6}$$

For $t \ge T_1$, from the second equation of system (3) and equation (6), we have:

$$\begin{aligned} \frac{dv}{dt} &= vF_2(u,v) \\ &\le sv\left(1 - \frac{v}{\beta\phi(\omega)(K+\varepsilon)+c}\right), \end{aligned}$$

By applying Lemma 2.3 in [25] to the aforementioned inequality, we derive:

$$\limsup_{t\to+\infty} v(t) \le \beta\phi(\omega)(K+\varepsilon) + c. \tag{7}$$

Because ε represents an arbitrarily small positive number, when we consider the limit as ε approaches 0 in equation (7), we get:

$$\limsup_{t\to+\infty} v(t) \le \beta\phi(\omega)K + c. \tag{8}$$

Equations (5) and (8) indicate that for the system (3) with initial conditions $u(0) > 0$ and $v(0) > 0$, the solutions and are uniformly bounded.

The proof of Theorem 2.2 is thus completed.

III. Existence Analysis of Equilibrium Points for System (3)

Regarding the existence of equilibrium points for system (3), we have the following result.

Theorem 3.1 *The vanishing equilibrium point $E_0(0,0)$, the prey-free equilibrium point $E_1(0,c)$, and the predator-free equilibrium point $E_2(K,0)$ always exist for system (3). Moreover, if and only if the following condition holds:*

$$r > \alpha\phi(\omega)c, \tag{9}$$

the system has a unique positive equilibrium point $E^*(u^*,v^*)$, where:

$$u^* = \frac{r - \alpha\phi(\omega)c}{\frac{r}{K} + \alpha\beta\phi^2(\omega)}, \quad v^* = \beta\phi(\omega)u^* + c. \tag{10}$$

Proof. The equilibrium points of system (3) satisfy the following equations:

$$\begin{aligned} uF_1(u,v) = 0, \\ vF_2(u,v) = 0. \end{aligned} \tag{11}$$

Considering the second equation in (11), we find that $v = 0$ or $v = \beta\phi(\omega)u + c$. When $v = 0$ is substituted into the first equation of (11), we obtain:

$$ru\left(1 - \frac{u}{K}\right) = 0 \tag{12}$$

The solutions to equation (12) are $u_1 = 0$ and $u_2 = K$. Therefore, system (3) has an vanishing equilibrium point $E_0(0,0)$ and a prey-free equilibrium point $E_2 = (K,0)$.

When we substitute $v = \beta\phi(\omega)u + c$ into the first equation of (11), the following is obtained:

$$ru\left(1 - \frac{u}{K}\right) - \alpha\phi(\omega)u\big(\beta\phi(\omega)u + c\big) = 0 \tag{13}$$

Obviously, system (13) has a solution $u = 0$, consequently, system (3) admits a prey-free equilibrium point $E_1 = (0,c)$. Under the condition (9), equation (13) has a unique positive solution u^*, where u^* is given by (10). Consequently, in system (3), there exists exactly one positive equilibrium point $E^*(u^*,v^*)$.

Hereby, the proof of Theorem 3.1 reaches its conclusion.

IV. Local Stability Analysis of Equilibrium Points for System (3)

Theorem 4.1 *The local stability conclusions for the equilibrium points of the system (3) are as follows:*

The vanishing equilibrium point $E_0(0,0)$ always unstable.

The predator-free equilibrium point $E_1(0,c)$ stable when $r < \alpha\phi(\omega)c$.

The prey-free equilibrium point $E_2(K,0)$ always unstable.

The positive equilibrium point $E^*(u^*,v^*)$ is always locally asymptotically stable when it exists ($r > \alpha\phi(\omega)c$).

proof The Jacobian matrix of system (3) is given by:

$$J(u,v) = \begin{pmatrix} \frac{\partial f}{\partial u} & \frac{\partial f}{\partial v} \\ \frac{\partial g}{\partial u} & \frac{\partial g}{\partial v} \end{pmatrix},$$

where:

$$\begin{aligned} \frac{\partial f}{\partial u} &= r\left(1-\frac{2u}{K}\right) - \alpha\phi(\omega)v, \\ \frac{\partial f}{\partial v} &= -\alpha\phi(\omega)u, \\ \frac{\partial g}{\partial u} &= \frac{s\beta\phi(\omega)v^2}{(\beta\phi(\omega)u+c)^2}, \\ \frac{\partial g}{\partial v} &= s\left(1-\frac{2v}{\beta\phi(\omega)u+c}\right). \end{aligned}$$

1) **The vanishing equilibrium point** $E_0 = (0,0)$:
The Jacobian matrix is:
$$J(E_0) = \begin{pmatrix} r & 0 \\ 0 & s \end{pmatrix}.$$
The eigenvalues are $\lambda_1 = r > 0$ and $\lambda_2 = s > 0$. Hence, E_0 is always an unstable source, indicating that the simultaneous extinction of both populations is impossible in the system (3).
2) **The predator-free equilibrium point** $E_1 = (0,c)$:
The Jacobian matrix is:
$$J(E_1) = \begin{pmatrix} r-\alpha\phi(\omega)c & 0 \\ s\beta\phi(\omega) & -s \end{pmatrix}.$$
The eigenvalues are $\lambda_1 = r - \alpha\phi(\omega)c$ and $\lambda_2 = -s < 0$. The stability condition is:
   - E_1 is locally asymptotically stable if $r < \alpha\phi(\omega)c$; otherwise, it is unstable.
3) **The prey-free equilibrium point** $E_2 = (K,0)$:
The Jacobian matrix is:
$$J(E_2) = \begin{pmatrix} -r & -\alpha\phi(\omega)K \\ 0 & s \end{pmatrix}.$$
The eigenvalues are $\lambda_1 = -r < 0$ and $\lambda_2 = s > 0$. Thus, E_2 is always an unstable saddle point, indicating that prey populations cannot survive while predator populations become extinct.
4) **The positive equilibrium point** $E^* = (u^*,v^*)$:
The Jacobian matrix is:
$$J(E^*) = \begin{pmatrix} -\frac{ru^*}{K} & -\alpha\phi(\omega)u^* \\ s\beta\phi(\omega) & -s \end{pmatrix}.$$
The trace and determinant are:
$$Tr(J) = -\frac{ru^*}{K} - s < 0,$$
$$Det(J) = \frac{ru^*s}{K} + \alpha\beta\phi^2(\omega)su^* > 0.$$
In light of the Routh-Hurwitz criterion, the positive equilibrium E^* is invariably locally asymptotically stable provided that $r > \alpha\phi(\omega)c$.

Thus, the proof of Theorem 4.1 comes to an end.

V. Extinction Analysis

In the preceding section, we demonstrated that the boundary equilibrium points E_0 and E_2 are unstable, while the boundary equilibrium point E_1 and the positive equilibrium point E^* are locally stable under appropriate conditions. A natural question is whether we can further explore their global stability. This section aims to identify sufficient conditions ensuring the global asymptotic stability of the prey-free equilibrium point $E_2(0,c)$. We have achieved the following result.

Theorem 5.1 *Under the condition*

$$r < \alpha\phi(\omega)c, \tag{14}$$

the prey-free equilibrium point $E_2(0,c)$ is globally attractive.

Proof. For a sufficiently small $\varepsilon > 0$, for the sake of generality, assume

$$0 < \varepsilon < c - \frac{r}{\alpha\phi(\omega)} \tag{15}$$

Then, one can conclude from inequality (14) that

$$r < \alpha\phi(\omega)(c-\varepsilon) \tag{16}$$

From the second equation of system (3) and the positivity of the solutions, we have

$$\begin{aligned} \tfrac{dv}{dt} &= vF_2(u,v) \\ &\geq sv\left(1-\tfrac{v}{c}\right). \end{aligned} \tag{17}$$

By applying Lemma 2.3 from [25] to the aforesaid inequality, we arrive at

$$\liminf_{t\to+\infty} v(t) \geq c. \tag{18}$$

Given any arbitrarily small $\varepsilon > 0$ that satisfies (15), there is a $T_1 > 0$ for which, for every $t > T_1$,

$$v(t) > c - \varepsilon. \tag{19}$$

For $t > T_1$, from the first equation of (3), it follows that

$$\begin{aligned} \tfrac{du}{dt} &= ru\left(1-\tfrac{u}{K}\right) - \alpha\phi(\omega)uv \\ &\leq ru\left(1-\tfrac{u}{K}\right) - \alpha\phi(\omega)u(c-\varepsilon) \\ &\leq \big(r - \alpha\phi(\omega)(c-\varepsilon)\big)u. \end{aligned} \tag{20}$$

Hence, for $t \geq T_1$,

$$u(t) \leq u(T_1)\exp\Big\{\int_{T_1}^{t}\big(r-\alpha\phi(\omega)(c-\varepsilon)\big)(t-T_1)dt\Big\}.$$

Applying (16) leads to

$$\lim_{t\to+\infty} u(t) = 0. \tag{21}$$

For above $\varepsilon > 0$, there exists a $T_2 > T_1$, such that

$$u(t) < \varepsilon \text{ for all } t \geq T_2. \tag{22}$$

It follows from the second equation of (3) and (22) that

$$\begin{aligned} \frac{dv}{dt} &= sv\left(1-\frac{v}{\beta\phi(\omega)u+c}\right) \\ &\leq sv\left(1-\frac{v}{\beta\phi(\omega)\varepsilon+c}\right). \end{aligned} \tag{23}$$

Hence

$$\limsup_{t\to+\infty} v(t) \leq \beta\phi(\omega)\varepsilon + c. \tag{24}$$

Since ε is enough small positive constant, seeting $\varepsilon \to 0$ in (24) leads to

$$\limsup_{t\to+\infty} v(t) \leq c. \tag{25}$$

Combined with (18) and (26) leads to

$$\lim_{t\to+\infty} v(t) = c. \tag{26}$$

(21) and (26) shows that the prey-free equilibrium point $E_2(0,c)$ is globally attractive.

The proof of Theorem 5.1 is finished.

VI. Global Stability of the Positive Equilibrium Point $E^* = (u^*, v^*)$

This section aims to conduct a study on the global stability of the positive equilibrium point within the system (3). The following result can be obtained.

Theorem 6.1 *If the following condition holds:*

$$r > \alpha\phi(\omega)c \tag{27}$$

then the positive equilibrium point $E_3(u^*, v^*)$ is globally asymptotically stable.

proof Provided that $r > \alpha\phi(\omega)c$, the positive equilibrium point exists and is locally asymptotically stable.

Below, we further prove its global stability.

Construct a Volterra-type Lyapunov function:

$$V(u,v) = \int_{u^*}^{u} \frac{\xi-u^*}{\xi}d\xi + a\int_{v^*}^{v}\frac{\eta-v^*}{\eta}d\eta,$$

where $a > 0$ is a parameter to be determined. Compute its derivative along the system trajectories:

$$\begin{aligned} \frac{dV}{dt} &= \left(1-\frac{u^*}{u}\right)\frac{du}{dt} + a\left(1-\frac{v^*}{v}\right)\frac{dv}{dt} \\ &= (u-u^*)\left[r\left(1-\frac{u}{K}\right)-\alpha\phi(\omega)v\right] \\ &\quad +a(v-v^*)\left[s\left(1-\frac{v}{\beta\phi(\omega)u+c}\right)\right]. \end{aligned}$$

Substituting the equilibrium conditions

$$r\left(1-\frac{u^*}{K}\right) = \alpha\phi(\omega)v^*$$

and

$$v^* = \beta\phi(\omega)u^* + c,$$

and simplifying, we obtain:

$$\begin{aligned} \frac{dV}{dt} &= -\frac{r}{K}(u-u^*)^2 - as\frac{(v-v^*)^2}{\beta\phi(\omega)u+c} \\ &\quad +\Big[\alpha\phi(\omega)(u-u^*)(v-v^*) \\ &\quad -as\beta\phi(\omega)\frac{(v-v^*)(u-u^*)}{\beta\phi(\omega)u+c}\Big]. \end{aligned}$$

Choose $a = \frac{\alpha\phi(\omega)(\beta\phi(\omega)u^*+c)}{\beta\phi(\omega)}$ to eliminate the cross terms. Then:

$$\frac{dV}{dt} = -\frac{r}{K}(u-u^*)^2 - \frac{\alpha\phi(\omega)s}{\beta\phi(\omega)u+c}(v-v^*)^2 \leq 0.$$

By LaSalle's invariance principle, the maximal invariant set is $\{(u^*, v^*)\}$. Therefore, E^* is globally asymptotically stable.

This completes the proof of Theorem 6.1.

Remark 6.1 Based on Theorem 6.1, it is globally asymptotically stable once the positive equilibrium point exists. In other words, system (3) does not exhibit bifurcation at E_3.

VII. Uniform persistence

A system is said to be persistent if, for any initial condition $(u(0), v(0)) \in R^+ \times R^+$, there exists a constant $\delta > 0$ such that:

$$\liminf_{t\to+\infty} u(t) \geq \delta, \quad \liminf_{t\to+\infty} v(t) \geq \delta.$$

Regarding the persistence of system (3), we have the following theorem.

Theorem 7.1 *If $r > \alpha\phi(\omega)c$, then system (3) is persistent.*

Proof From Theorem 2.2, the solutions of the system satisfy:

$$\limsup_{t\to+\infty} u(t) \leq K, \quad \limsup_{t\to+\infty} v(t) \leq \beta\phi(\omega)K + c.$$

Thus, the solutions always remain within the region $\Omega = [0,K] \times [0, \beta\phi(\omega)K + c]$. Next, we exclude boundary attractors, i.e., we need to prove that no trajectories within Ω tend to the boundary equilibrium points. Consider the following two cases:

- **Prey Extinction**: If $r < \alpha\phi(\omega)c$, then E_1 is globally stable, and the prey population goes extinct. However, the current condition is $r > \alpha\phi(\omega)c$, so E_1 is unstable.
- **Predator Extinction**: E_2 is always a saddle point, and its stable manifold lies on the $v = 0$ axis. However, the initial values of the system solutions are in $R^+ \times R^+$, so the solutions will not tend to E_2 along this manifold.

Now let us consider the average Lyapunov function

$$P(u,v) = u^\theta v^\eta,$$

where $\theta, \eta > 0$ are weight parameters. Let

$$\theta = \frac{\eta\beta\phi(\omega)v^*}{\alpha\phi(\omega)u^*(\beta\phi(\omega)u^*+c)}.$$

Taking the derivative of $P(u,v)$ concerning time t, according to the chain - rule for composite functions,

$$\frac{dP}{dt} = \frac{\partial P}{\partial u}\frac{du}{dt} + \frac{\partial P}{\partial v}\frac{dv}{dt}.$$

We have:

$$\begin{aligned}\frac{dP}{dt} &= \theta u^{\theta-1}v^{\eta}\left(ru(1-\tfrac{u}{K})-\alpha\phi(\omega)uv\right)\\ &\quad+\eta u^{\theta}v^{\eta-1}\left(sv(1-\tfrac{v}{\beta\phi(\omega)u+c})\right)\\ &= \theta u^{\theta}v^{\eta}\left(r(1-\tfrac{u}{K})-\alpha\phi(\omega)v\right)\\ &\quad+\eta u^{\theta}v^{\eta}\left(s(1-\tfrac{v}{\beta\phi(\omega)u+c})\right)\\ &= u^{\theta}v^{\eta}\Big[\theta\left(r(1-\tfrac{u}{K})-\alpha\phi(\omega)v\right)\\ &\quad+\eta\left(s(1-\tfrac{v}{\beta\phi(\omega)u+c})\right)\Big] \qquad (28)\\ &= u^{\theta}v^{\eta}\Bigg[\frac{\eta s\beta\phi(\omega)v^{*}r}{\alpha\phi(\omega)u^{*}(\beta\phi(\omega)u^{*}+c)}\\ &\quad-\frac{\eta s\beta\phi(\omega)v^{*}ru}{K\alpha\phi(\omega)u^{*}(\beta\phi(\omega)u^{*}+c)}\\ &\quad-\frac{\eta s\beta\phi(\omega)v^{*}\alpha\phi(\omega)v}{\alpha\phi(\omega)u^{*}(\beta\phi(\omega)u^{*}+c)}\\ &\quad+\eta s-\frac{\eta sv}{\beta\phi(\omega)u+c}\Bigg]\end{aligned}$$

Because the positive equilibrium point E^{*} meets the condition

$$r(1-\frac{u^{*}}{K})=\alpha\phi(\omega)v^{*},$$

namely,

$$r-\frac{ru^{*}}{K}=\alpha\phi(\omega)v^{*},$$

then

$$\begin{aligned}&\frac{\eta s\beta\phi(\omega)v^{*}r}{\alpha\phi(\omega)u^{*}(\beta\phi(\omega)u^{*}+c)}\\ =\;&\frac{\eta s\beta\phi(\omega)}{\alpha\phi(\omega)u^{*}(\beta\phi(\omega)u^{*}+c)}(r-\frac{ru^{*}}{K}).\end{aligned} \qquad (29)$$

Substitute it into the above formula and simplify:

$$\begin{aligned}&\frac{dP}{dt}\\ =\;&u^{\theta}v^{\eta}\Bigg[\frac{\eta s\beta\phi(\omega)}{\alpha\phi(\omega)u^{*}(\beta\phi(\omega)u^{*}+c)}\left(r-\frac{ru^{*}}{K}\right)\\ &-\frac{\eta s\beta\phi(\omega)v^{*}ru}{K\alpha\phi(\omega)u^{*}(\beta\phi(\omega)u^{*}+c)}\\ &-\frac{\eta s\beta\phi(\omega)v^{*}\alpha\phi(\omega)v}{\alpha\phi(\omega)u^{*}(\beta\phi(\omega)u^{*}+c)}\\ &+\eta s-\frac{\eta sv}{\beta\phi(\omega)u+c}\Bigg]\\ =\;&u^{\theta}v^{\eta}\Bigg[\frac{\eta s\beta\phi(\omega)r}{\alpha\phi(\omega)u^{*}(\beta\phi(\omega)u^{*}+c)}\\ &-\frac{\eta s\beta\phi(\omega)ru^{*}}{K\alpha\phi(\omega)u^{*}(\beta\phi(\omega)u^{*}+c)}\\ &-\frac{\eta s\beta\phi(\omega)v^{*}ru}{K\alpha\phi(\omega)u^{*}(\beta\phi(\omega)u^{*}+c)}\\ &-\frac{\eta s\beta\phi(\omega)v^{*}\alpha\phi(\omega)v}{\alpha\phi(\omega)u^{*}(\beta\phi(\omega)u^{*}+c)}\\ &+\eta s-\frac{\eta sv}{\beta\phi(\omega)u+c}\Bigg]\end{aligned} \qquad (30)$$

Because $u\in(0,K]$, so

$$\frac{\eta s\beta\phi(\omega)v^{*}ru}{K\alpha\phi(\omega)u^{*}(\beta\phi(\omega)u^{*}+c)}\le\frac{\eta s\beta\phi(\omega)v^{*}r}{\alpha\phi(\omega)u^{*}(\beta\phi(\omega)u^{*}+c)}.$$

And because $v\in(0,\beta\phi(\omega)K+c]$, then

$$\frac{\eta s\beta\phi(\omega)v^{*}\alpha\phi(\omega)v}{\alpha\phi(\omega)u^{*}(\beta\phi(\omega)u^{*}+c)}\le\frac{\eta s\beta\phi(\omega)v^{*}\alpha\phi(\omega)(\beta\phi(\omega)K+c)}{\alpha\phi(\omega)u^{*}(\beta\phi(\omega)u^{*}+c)}$$

and

$$\frac{\eta sv}{\beta\phi(\omega)u+c}\le\frac{\eta s(\beta\phi(\omega)K+c)}{\beta\phi(\omega)u+c}.$$

One can observe that

$$\begin{aligned}&\frac{dP}{dt}\\ \ge\;&u^{\theta}v^{\eta}\Big[\frac{\eta s\beta\phi(\omega)r}{\alpha\phi(\omega)u^{*}(\beta\phi(\omega)u^{*}+c)}\\ &-\frac{\eta s\beta\phi(\omega)ru^{*}}{K\alpha\phi(\omega)u^{*}(\beta\phi(\omega)u^{*}+c)}\\ &-\frac{\eta s\beta\phi(\omega)v^{*}r}{\alpha\phi(\omega)u^{*}(\beta\phi(\omega)u^{*}+c)}\\ &-\frac{\eta s\beta\phi(\omega)v^{*}\alpha\phi(\omega)(\beta\phi(\omega)K+c)}{\alpha\phi(\omega)u^{*}(\beta\phi(\omega)u^{*}+c)}\\ &+\eta s-\frac{\eta s(\beta\phi(\omega)K+c)}{\beta\phi(\omega)u+c}\Big] \qquad (31)\\ \ge\;&u^{\theta}v^{\eta}\Bigg[\eta s-\frac{\eta s\beta\phi(\omega)ru^{*}}{K\alpha\phi(\omega)u^{*}(\beta\phi(\omega)u^{*}+c)}\\ &-\frac{\eta s\beta\phi(\omega)v^{*}\alpha\phi(\omega)(\beta\phi(\omega)K+c)}{\alpha\phi(\omega)u^{*}(\beta\phi(\omega)u^{*}+c)}\\ &-\frac{\eta s(\beta\phi(\omega)K+c)}{\beta\phi(\omega)u+c}\Bigg].\end{aligned}$$

Given that $u^{*}=\frac{r-\alpha\phi(\omega)c}{\frac{r}{K}+\alpha\beta\phi^{2}(\omega)}>0$ and $r>\alpha\phi(\omega)c$, we can conclude that

$$\beta\phi(\omega)u^{*}+c<\beta\phi(\omega)K+c.$$

So

$$1-\frac{\beta\phi(\omega)K+c}{\beta\phi(\omega)u^{*}+c}>0.$$

Let

$$M=\eta s\Big(1-\frac{\beta\phi(\omega)K+c}{\beta\phi(\omega)u^{*}+c}\Big).$$

Because $\eta>0$, $s>0$, and $1-\frac{\beta\phi(\omega)K+c}{\beta\phi(\omega)u^{*}+c}>0$, then $M>0$. Then when t is large enough, $\frac{dP}{dt}\ge Mu^{\theta}v^{\eta}>0$ (because $u^{\theta}v^{\eta}>0$, $u>0$, $v>0$). This indicates that as time t increases, $P(u,v)$ will not approach 0. Since $P(u,v)=u^{\theta}v^{\eta}$, both u and v will not approach 0.

According to the definition of persistence, for any initial conditions $(u(0),v(0))\in R^{+}\times R^{+}$, to prove that system (3) is persistent, there needs to exist a constant $\delta>0$ such that $\liminf_{t\to+\infty}u(t)\ge\delta$ and $\liminf_{t\to+\infty}v(t)\ge\delta$.

Since it has been proven that when t is large enough, $\frac{dP}{dt}\ge Mu^{\theta}v^{\eta}>0$, this shows that $P(u,v)=u^{\theta}v^{\eta}$ will not approach 0 as time t increases.

Next, choose δ such that $0<\delta^{\theta+\eta}<\frac{M}{2}$. Suppose there exists a time T such that when $t>T$, $u^{\theta}v^{\eta}<\delta^{\theta+\eta}$. Because $\frac{dP}{dt}\ge Mu^{\theta}v^{\eta}$, at this time $\frac{dP}{dt}>0$, which means that $P(u,v)=u^{\theta}v^{\eta}$ is monotonically increasing when $t>T$. So $u^{\theta}v^{\eta}$ will not continuously be less than $\delta^{\theta+\eta}$, that is,

$u^\theta v^\eta$ will necessarily be greater than or equal to $\delta^{\theta+\eta}$. And because $\theta > 0$, $\eta > 0$, according to the properties of exponential functions, it can be obtained that $u \geq \delta$ and $v \geq \delta$. So $\liminf_{t\to+\infty} u(t) \geq \delta$ and $\liminf_{t\to+\infty} v(t) \geq \delta$, which satisfies the definition of the persistence of system (3). Thus, system (3) is persistent

The proof of Theorem 7.1 is complete.

VIII. Transcritical Bifurcation

This section explores the bifurcation behavior of the system. We have the following result.

Theorem 8.1 *Consider system (3) with the saturation function $\phi(\omega) = 1 + \frac{\omega}{k+\omega}$. Under the parameter constraint:*

$$\alpha c < r < 2\alpha c,$$

the system undergoes a transcritical bifurcation at the boundary equilibrium $E_1(0, c)$ when the wind speed reaches the critical value:

$$\omega_c = \frac{k(r - \alpha c)}{2\alpha c - r}.$$

The bifurcation exhibits the following properties:

1) *For $\omega < \omega_c$, the positive equilibrium E^* exists and is globally asymptotically stable.*
2) *For $\omega > \omega_c$, E^* vanishes, and the boundary equilibrium $E_1(0, c)$ becomes stable.*
3) *At $\omega = \omega_c$, E^* collides with $E_1(0, c)$, exchanging stability.*

Proof. We divide the proof of this theorem into four steps.

Step 1: Derivation of Critical Wind Speed

The existence condition for the positive equilibrium E^* is:

$$r > \alpha\phi(\omega)c.$$

At bifurcation, E^* coincides with $E_1(0, c)$, implying:

$$r = \alpha\phi(\omega_c)c.$$

Substituting $\phi(\omega_c) = 1 + \frac{\omega_c}{k+\omega_c}$:

$$r = \alpha c\left(1 + \frac{\omega_c}{k + \omega_c}\right).$$

Solving for ω_c:

$$\omega_c = \frac{k(r - \alpha c)}{2\alpha c - r}.$$

The physical constraint $\omega_c > 0$ requires $\alpha c < r < 2\alpha c$.

Step 2: Jacobian Matrix and Eigenvalue Analysis The Jacobian matrix at $E_1(0, c)$ is:

$$J(E_1) = \begin{pmatrix} r - \alpha\phi(\omega)c & 0 \\ s\beta\phi(\omega) & -s \end{pmatrix}.$$

At $\omega = \omega_c$, substituting $r = \alpha\phi(\omega_c)c$:

$$J(E_1, \omega_c) = \begin{pmatrix} 0 & 0 \\ s\beta\phi(\omega_c) & -s \end{pmatrix}.$$

The eigenvalues are $\lambda_1 = 0$ and $\lambda_2 = -s < 0$, confirming the necessary condition for bifurcation.

Step 3: Right and Left Eigenvectors

From $J(E_1, \omega_c)V = 0$, we have:

$$0 \cdot V_1 + 0 \cdot V_2 = 0,$$
$$s\beta\phi(\omega_c)V_1 - sV_2 = 0.$$

Let $V_1 = 1$, then $V_2 = \beta\phi(\omega_c)$. Therefore:

$$V = \begin{pmatrix} 1 \\ \beta\phi(\omega_c) \end{pmatrix}.$$

From $WJ(E_1, \omega_c) = 0$, we have:

$$W_1 \cdot 0 + W_2 \cdot s\beta\phi(\omega_c) = 0,$$
$$W_1 \cdot 0 + W_2 \cdot (-s) = 0.$$

Let $W_1 = 1$, then $W_2 = 0$. Therefore:

$$W = (1, 0).$$

Step 4: Verification of Transversality (Sotomayor's Theorem)

The system's equations are:

$$\begin{aligned} \tfrac{du}{dt} &= ru\left(1 - \tfrac{u}{K}\right) - \alpha\phi(\omega)uv \stackrel{\text{def}}{=} f_1(u, v), \\ \tfrac{dv}{dt} &= sv\left(1 - \tfrac{v}{\beta\phi(\omega)u+c}\right) \stackrel{\text{def}}{=} f_2(u, v). \end{aligned}$$

The partial derivative of f with respect to ω at $E_1(0, c)$ is:

$$\left.\frac{\partial f}{\partial \omega}\right|_{(E_1,\omega_c)} = \left.\begin{pmatrix} -\alpha\frac{\partial\phi}{\partial\omega} \cdot uv \\ s\beta\frac{\partial\phi}{\partial\omega} \cdot \frac{v^2}{\beta\phi(\omega)u+c} \end{pmatrix}\right|_{(0,c)}.$$

Substituting $\phi(\omega) = 1 + \frac{\omega}{k+\omega}$ and $\frac{\partial\phi}{\partial\omega} = \frac{k}{(k+\omega)^2}$:

$$\begin{aligned} \left.\tfrac{\partial f}{\partial\omega}\right|_{(E_1,\omega_c)} &= \begin{pmatrix} -\alpha c \cdot \frac{k}{(k+\omega_c)^2} \cdot 0 \\ s\beta \cdot \frac{k}{(k+\omega_c)^2} \cdot \frac{c^2}{c} \end{pmatrix} \\ &= \begin{pmatrix} 0 \\ s\beta\frac{kc}{(k+\omega_c)^2} \end{pmatrix}. \end{aligned}$$

Left-multiplying by $W = (1, 0)$:

$$W^T \cdot \left.\frac{\partial f}{\partial\omega}\right|_{(E_1,\omega_c)} = 0.$$

The parameter derivative matrix $D\left(\frac{\partial f}{\partial\omega}\right)$ is computed as:

$$\begin{aligned} &D\left(\tfrac{\partial f}{\partial\omega}\right) \\ &= \begin{pmatrix} -\alpha\frac{k}{(k+\omega)^2}v & -\alpha\frac{k}{(k+\omega)^2}u \\ s\beta\frac{k}{(k+\omega)^2} \cdot \frac{2v}{\beta\phi(\omega)u+c} & s\beta\frac{k}{(k+\omega)^2} \cdot \frac{u^2}{(\beta\phi(\omega)u+c)^2} \end{pmatrix}. \end{aligned}$$

At the boundary equilibrium $E_1(0, c)$, substituting $u = 0$ and $v = c$:

$$D\left(\frac{\partial f}{\partial\omega}\right)\Big|_{(E_1,\omega_c)} = \begin{pmatrix} -\alpha\frac{kc}{(k+\omega_c)^2} & 0 \\ 2s\beta\frac{k}{(k+\omega_c)^2} & 0 \end{pmatrix}.$$

Multiplying by the right eigenvector $V = \begin{pmatrix} 1 \\ \beta\phi(\omega_c) \end{pmatrix}$:

$$D\left(\frac{\partial f}{\partial\omega}\right)V = \begin{pmatrix} -\alpha\frac{kc}{(k+\omega_c)^2} \\ 2s\beta\frac{k}{(k+\omega_c)^2} \end{pmatrix}.$$

Left-multiplying by the left eigenvector $W = (1, 0)$:

$$W^T \cdot D\left(\frac{\partial f}{\partial\omega}\right)V = -\alpha\frac{kc}{(k + \omega_c)^2} \neq 0.$$

The second derivative $D^2 f(V, V)$ is computed as:

$$D^2 f(V, V) = \begin{pmatrix} \sum_{i,j}\frac{\partial^2 f_1}{\partial u_i \partial u_j}V_iV_j \\ \sum_{i,j}\frac{\partial^2 f_2}{\partial u_i \partial u_j}V_iV_j \end{pmatrix}.$$

For f_1:

$$\frac{\partial^2 f_1}{\partial u^2} = -\frac{2r}{K}, \quad \frac{\partial^2 f_1}{\partial u \partial v} = -\alpha\phi(\omega), \quad \frac{\partial^2 f_1}{\partial v^2} = 0.$$

For f_2:

$$\frac{\partial^2 f_2}{\partial u^2} = \frac{2s\beta^2\phi^2 v^2}{(\beta\phi u + c)^3},$$
$$\frac{\partial^2 f_2}{\partial u \partial v} = -\frac{2s\beta\phi v}{(\beta\phi u + c)^2},$$
$$\frac{\partial^2 f_2}{\partial v^2} = -\frac{2s}{\beta\phi u + c}.$$

At $E_1(0, c)$, substituting $V = \begin{pmatrix} 1 \\ \beta\phi(\omega_c) \end{pmatrix}$:

$$D^2 f(V, V) = \begin{pmatrix} -\frac{2r}{K} - 2\alpha\beta\phi^2(\omega_c) \\ -\frac{2s\beta^2\phi^2(\omega_c)}{c} \end{pmatrix}.$$

Left-multiplying by the left eigenvector $W = (1, 0)$:

$$W^T \cdot D^2 f(V, V) = -\frac{2r}{K} - 2\alpha\beta\phi^2(\omega_c) \neq 0.$$

According to Sotomayor's theorem, the system satisfies all conditions for a transcritical bifurcation at $\omega = \omega_c$. When $\omega < \omega_c$, the positive equilibrium point E^* exists and is stable; when $\omega > \omega_c$, E^* disappears, and the boundary equilibrium point $E_1(0, c)$ becomes stable. The system undergoes a transcritical bifurcation, and the equilibrium points exchange stability.

This ends the proof of Theorem 8.1.

Remark 8.1. Ecological Significance:
The critical wind speed ω_c reflects the regulatory effect of wind speed on the predator-prey system:

- **Low Wind Speed** ($\omega < \omega_c$): Predation pressure increases with wind speed, but the system maintains a coexistence state.
- **High Wind Speed** ($\omega > \omega_c$): Predation pressure saturates, leading to the extinction of the prey population, and the system tends toward a stable state where the predator relies on external resources c.

Theorem 8.1 provides a theoretical basis for predicting state transitions in ecosystems under climate change.

IX. Dynamical Analysis of Saturation Wind Effects

In this section, we conduct a theoretical analysis to systematically explore the impact of saturation wind effects on the system's dynamical behavior. Specifically, we investigate the mathematical properties of the saturation function $\phi(\omega)$, the influence of wind speed on predation rate and predator carrying capacity, and the existence of a critical wind speed ω_c along with its ecological implications.

A. Properties of the Saturation Function $\phi(\omega)$

The saturation function $\phi(\omega) = 1 + \frac{\omega}{k+\omega}$ is central to our model, describing the nonlinear impact of wind speed ω on predation rate and predator carrying capacity. This function exhibits the following key properties:

- **Low Wind Speed Behavior**: As $\omega \to 0$, $\phi(\omega) \approx 1 + \frac{\omega}{k}$, indicating that the effect of wind speed on the system is approximately linear. In this regime, an increase in wind speed significantly enhances predation rate and predator carrying capacity.
- **High Wind Speed Saturation**: As $\omega \to \infty$, $\phi(\omega) \to 2$, indicating that the effect of wind speed saturates. In this regime, further increases in wind speed do not significantly affect predation rate or predator carrying capacity.
- **Role of the Parameter** k: The parameter k is the half-saturation constant, representing the wind speed at which the effect reaches half of its maximum. A smaller k implies that the system reaches saturation at lower wind speeds, while a larger k implies a slower response to changes in wind speed.

B. Effect of Wind Speed on Predation Rate

The predation rate $\alpha\phi(\omega)u$ is a key mechanism through which wind speed influences the system dynamics. By analyzing the properties of $\phi(\omega)$, we derive the following conclusions:

- **At Low Wind Speeds**: When $\omega \ll k$, the predation rate $\alpha\phi(\omega)u \approx \alpha\left(1 + \frac{\omega}{k}\right)u$, indicating that predation rate increases approximately linearly with wind speed.
- **At High Wind Speeds**: When $\omega \gg k$, the predation rate $\alpha\phi(\omega)u \approx 2\alpha u$, indicating that predation rate saturates and no longer increases significantly with wind speed.

This saturation effect reflects the adaptive strategies of organisms to extreme environmental conditions. An increase in wind speed enhances predator efficiency at low wind speeds, while at high wind speeds, physical limitations prevent further increases in predation efficiency.

C. Effect of Wind Speed on Predator Carrying Capacity

The predator carrying capacity $\beta\phi(\omega)u + c$ is also influenced by wind speed. By analyzing the properties of $\phi(\omega)$, we derive the following conclusions:

- **At Low Wind Speeds**: When $\omega \ll k$, the predator carrying capacity $\beta\phi(\omega)u + c \approx \beta\left(1 + \frac{\omega}{k}\right)u + c$, indicating that carrying capacity increases approximately linearly with wind speed.
- **At High Wind Speeds**: When $\omega \gg k$, the predator carrying capacity $\beta\phi(\omega)u + c \approx 2\beta u + c$, indicating that carrying capacity saturates and is primarily determined by prey resources u.

This saturation effect suggests that predator carrying capacity no longer increases significantly at high wind speeds, and predator population size is primarily dependent on prey resources.

D. Existence of Critical Wind Speed ω_c

Through theoretical analysis, we derive the expression for the critical wind speed ω_c:

$$\omega_c = \frac{k(r - \alpha c)}{2\alpha c - r}$$

The critical wind speed ω_c is the threshold at which the system transitions from a coexistence state (positive equilibrium E^*) to a prey extinction state (boundary equilibrium $E_1(0, c)$). The existence condition for ω_c is:

$$\alpha c < r < 2\alpha c$$

- **When** $\omega < \omega_c$: The system has a unique positive equilibrium E^*, which is locally asymptotically stable, indicating that predators and prey can coexist.
- **When** $\omega > \omega_c$: The positive equilibrium E^* disappears, and the system tends toward prey extinction, with predators relying on external resources c to sustain their population.

The discovery of ω_c reveals the critical role of wind speed in ecosystem state transitions. When wind speed exceeds the critical value, predation pressure saturates, leading to prey extinction and a new stable state for the system.

E. Regulatory Role of the Parameter k

The parameter k, as the half-saturation constant, plays a crucial role in regulating the system's sensitivity to wind speed:

- **Small** k: The system reaches saturation at lower wind speeds, indicating higher sensitivity to wind speed changes. This property is suitable for fragile ecosystems (e.g., grasslands) easily disturbed by wind.
- **Large** k: The system responds more slowly to wind speed changes, requiring higher wind speeds to reach saturation. This property is suitable for stable ecosystems (e.g., forests) less sensitive to wind speed variations.

Adjusting the parameter k can optimize ecological management strategies. For example, increasing vegetation density in agricultural ecosystems can reduce local wind speed, thereby enhancing predator efficiency and controlling pest populations.

X. Numerical Simulations

Example 10.1 Take the following model into consideration:

$$\begin{aligned} \frac{du}{dt} &= 8u\Big(1-\frac{u}{10}\Big) - 0.5 \times \Big(1+\frac{2}{1+2}\Big)uv, \\ \frac{dv}{dt} &= v\left(1-\frac{v}{3u \times (1+\frac{2}{1+2})+1}\right), \end{aligned} \tag{32}$$

where, corresponding to system (3), we set $r = 8$, $K = 10$, $\alpha = 0.5$, $s = 1$, $\beta = 3$, $c = 1$, and $\omega = 2$. Here, $\phi(\omega) = \frac{\omega}{1+\omega}$. Calculations show that:

$$r = 8 > \frac{5}{6} = \alpha c\phi(\omega), \tag{33}$$

and by Theorem 6.1 and Theorem 7.1, the positive equilibrium point $E^*(u^*, v^*) \approx (1.442953020, 8.214765100)$ is globally asymptotically stable, and the system demonstrates persistence. The numerical simulation presented in Figure 1 validates this finding.

Example 10.2 Take into account the following model:

$$\begin{aligned} \frac{du}{dt} &= u\Big(1-\frac{u}{10}\Big) - 2 \times \Big(1+\frac{3}{1+3}\Big)uv, \\ \frac{dv}{dt} &= v\left(1-\frac{v}{3u\Big(1+\frac{3}{1+3}\Big)+1}\right), \end{aligned} \tag{34}$$

where, corresponding to the system (3), we set $r = 1$, $K = 10$, $\alpha = 2$, $\beta = 3$, $c = 1$, $\omega = 3$, and $k = 1$. Note that $r = 1 < \frac{7}{2} = \alpha c\phi(\omega)$, satisfying the condition of Theorem 5.1. According to Theorem 5.1, the boundary equilibrium point $E_2(0, 1)$ is globally asymptotically stable. Numerical simulation (Figure 2) supports this conclusion.

Example 10.3 Give thought to the following model:

$$\begin{aligned} \frac{du}{dt} &= 2u\Big(1-\frac{u}{100}\Big) - 0.5 \times \Big(1+\frac{\omega}{k+\omega}\Big)uv, \\ \frac{dv}{dt} &= v\left(1-\frac{v}{0.1 \times u \times \Big(1+\frac{\omega}{k+\omega}\Big)+3}\right), \end{aligned} \tag{35}$$

where, corresponding to system (3), we set $r = 2$, $K = 100$, $\alpha = 0.5$, $s = 1$, $\beta = 0.1$, and $c = 3$.

(1) Corresponding to Theorem 8.1, one could see that $w_c = 1$ by simple computation. one could see that $w_c = 1$. We vary $\omega = 0, 0.1, 0.5, 1, 2$, then, from Theorem 8.1, for $\omega = 0, 0.1, 0.5$, $u(t) \to u^*_\omega$, and for $\omega \geq 1$(where 1 is the critical value), $u(t) \to 0$ as $t \to +\infty$. Take initial conditions $(u(0), v(0)) = (5, 3)$. Figure 3 shows the behavior of the first component $u(t)$ for different ω values. As ω increases, u^* gradually decreases, and when ω is sufficiently large, $u(t) \to 0$. That is, when wind speed is high enough, the prey population tends to extinction, and $v(t) \to c$. This is consistent with the theoretical analysis in Sections 8. Additionally, Figure 4 shows that as ω increases, the predator population density $v(t)$ tends to c. Figure 5 shows the bifurcation diagram of u^* with respect to ω. From the diagram, it can be observed that as ω increases, u^* gradually decreases. Eventually, when the wind speed crosses the critical value, u^* becomes zero. Figure 6 shows the bifurcation diagram of v^* with respect to ω. From the diagram, it can be observed that as ω increases, v^* gradually decreases. Eventually, when the wind speed crosses the critical value, $v^* = c$.

(2) In this case, we take $w = 0.5$ and vary k. Figure 7 and 8 show the bifurcation diagram of $u^*(k)$ and $v^*(k)$, respectively. From the diagram, it can be observed that as k increases, u^* gradually decreases, and if k is very small, $u(t)$ is very sensitive to k, and finally, $u(t) \to 0$. However, we could not find the similar phenomenon for $v^*(k)$.

(3) In this case, we vary both k and ω, Figure 9 and 10 show the bifurcation diagram of $u^*(k, \omega)$ and $v^*(k, \omega)$, respectively. From Figure 9, it can be observed that as k increases, the u population can tolerate the effects of wind over a wider range and ultimately sustain its survival. This situation similarly holds for $v^*(k)$.

Sensitivity analysis of parameter k (Fig. 7-10) reveals that smaller k accelerates the transition to prey extinction, suggesting ecosystems with low saturation thresholds are more vulnerable to wind-driven collapse.

Example 10.4 Give thought to the following model:

$$\begin{aligned} \frac{du}{dt} &= 5u\Big(1-\frac{u}{10}\Big) - 0.5 \times \phi(k,\omega)uv, \\ \frac{dv}{dt} &= v\left(1-\frac{v}{0.1 \times u \times \phi(k,\omega)+3}\right), \end{aligned} \tag{36}$$

where, corresponding to the system (3), we set $r = 5$, $K = 10$, $\alpha = 0.5$, $s = 1$, $\beta = 0.1$, and $c = 3$.
(1) In this case, we take $\phi(k, \omega) = 1 + \omega$, then it follows from Theorem 4.1, 5.1, and 6.1 of Huang et al.[18] that there exists a $\omega_c = 3$, and for $\omega > w_c$, the prey species will be driven to extinction. the predator species will approach to 3. Fig. 11 and 12 also confirm this assertion.
(2) In this case, we take $\phi(k, \omega) = \left(1 + \frac{\omega}{k+\omega}\right)$, then one could easily verify that $r = 6 > 2\alpha c = 3 > 2\alpha\phi(k, \omega)c$, hence, the system has positive equilibrium $E^*(u^*.v^*)$ for all k and ω. it follows from Theorem 4.1, 5.1, and 6.1 of Huang et al.[18] that there exists a $\omega_c = 3$, and for $\omega > w_c$,, the prey species will be driven to extinction. The predator species will approach 3. Fig. 13 and 14 also confirm this assertion.

This example vividly illustrates the stark contrast between the results of our study and those of reference [18]. In reference [18], due to the linear effect of wind speed on the interaction between the two populations, as wind speed increases, the impact of predators on the prey population becomes increasingly significant, ultimately leading to the extinction of the prey population. In contrast, in our study, because of the saturation effect of wind speed, as long as the interspecies coefficients satisfy certain conditions, both populations will coexist regardless of how large the wind speed becomes. Although wind speed affects the final equilibrium densities of the populations, the relationship is highly complex, as evidenced by Figures 13 and 14.

XI. Conclusion and Discussion

Recently, Jawad et al.[17] and Huang et al.[18] studied the influence of wind effect on predator prey system. Although the linear wind effect model ($\phi(\omega) = 1 + \omega$) proposed by Huang et al. [18] can explain the decline in prey population density with increasing wind speed, its assumption of unlimited growth in predation rate contradicts ecological reality. The model by Jawad et al.[17] even yields a counterintuitive conclusion that "increasing wind speed enhances the densities of both species," which conflicts with field observations[16]. Moreover, these models fail to account for organisms' adaptive strategies to extreme wind conditions (e.g., sheltering behavior or saturation of predation efficiency).

In this paper, we have proposed a **modified Leslie-Gower predator-prey model** incorporating **saturation wind effects** to explore the nonlinear impact of wind speed on ecosystem dynamics. Our study systematically reveals the multi-scale effects of wind speed on predation rate, predator carrying capacity, and ecosystem state transitions. Below, we summarize the key findings, ecological implications, and future research directions. Unlike Jawad et al. [17] where both populations grow with ω, our saturation effect explains why prey decline dominates at high winds – reconciling field observations [16].

Key Contributions:

1) **Saturation Wind Effects**: By introducing the saturation function $\phi(\omega) = 1 + \frac{\omega}{k+\omega}$, our model captures the nonlinear relationship between wind speed and predation rate. At low wind speeds, predation rate increases approximately linearly with wind speed, but saturates at high wind speeds, reflecting the adaptive strategies of organisms to extreme environmental conditions.
2) **Critical Wind Speed** (ω_c): We derived the critical wind speed $\omega_c = \frac{k(r-\alpha c)}{2\alpha c - r}$, which serves as a threshold for ecosystem state transitions. When wind speed exceeds ω_c, the system transitions from a **coexistence state** to **prey extinction**, with predators relying on external resources c to sustain their population.
3) **Regulatory Role of** k: The half-saturation constant k plays a crucial role in regulating the system's sensitivity to wind speed. Smaller k values make the system more sensitive to wind speed changes, while larger k values result in a slower response. This finding provides a theoretical basis for optimizing ecological management strategies, such as increasing vegetation density to reduce local wind speed and enhance predator efficiency.

Ecological Implications:

- **Wind Speed as a Key Factor**: Our results highlight the critical role of wind speed in predator-prey dynamics. The saturation effect reflects the adaptive behaviors of organisms to extreme environmental conditions, where predation pressure and predator carrying capacity no longer increase significantly at high wind speeds.
- **State Transitions in Ecosystems**: The critical wind speed ω_c provides a theoretical boundary for predicting ecosystem state transitions. When wind speed exceeds ω_c, the system transitions from coexistence to prey extinction, aligning with ecological observations in natural systems.
- **Applications in Ecological Management**: By adjusting habitat structures (e.g., vegetation density) to modify the local k value, ecological management strategies can be optimized. For example, increasing windbreaks in agricultural fields can enhance the predation efficiency of natural enemies, thereby improving pest control.

Limitations and Future Research:

While our model provides valuable insights into the impact of wind speed on predator-prey dynamics, several limitations and future research directions remain:

1) **Model Limitations**:Our model assumes that wind speed uniformly affects predation rate and predator carrying capacity. However, in reality, different species may respond differently to wind speed. Future work could incorporate species-specific responses to wind speed or extend the model to include multiple prey and predator species.
2) **Multi-Factor Coupling**: Future research could explore the combined effects of multiple environmental factors, such as temperature, humidity, and wind speed, on ecosystem dynamics. This would provide a more comprehensive understanding of how climate change influences species interactions.
3) **Spatial Heterogeneity**: Incorporating spatial heterogeneity into the model could reveal how wind speed variations across habitats affect predator-prey interactions. This would be particularly relevant for large-scale ecosystems with diverse environmental conditions.

4) **Experimental Validation**: Empirical studies are needed to validate the theoretical predictions of this model. Experimental data from field observations or controlled environments could help refine the model parameters and improve its applicability to real-world ecosystems.

Concluding Remarks:

In conclusion, this study offers a novel modeling framework for understanding the complex relationship between wind speed and predator-prey dynamics.We have demonstrated how wind speed influences predation rate, predator carrying capacity, and ecosystem state transitions by introducing saturation wind effects. The discovery of the critical wind speed ω_c and the regulatory role of the parameter k provide new tools for predicting and managing the impacts of wind speed on ecosystems. These findings have broad applications in ecological conservation, agricultural pest control, and climate change research, offering a foundation for future studies on the interplay between environmental factors and species interactions.

ACKNOWLEDGMENT

The authors wish to convey their thanks to Dr. Shireen Jawad for the communication.

This exchange drew our intense attention to the wind effect and inspired us to conduct relevant research.

REFERENCES

[1] X. Wang, L. Zanette, X. Zou, "Modelling the fear effect in predator-prey interactions," *Journal of Mathematical Biology,* vol.73, no. 5, pp. 1179-1204, 2016.

[2] X. Wang, X. Zou, "Modeling the fear effect in predator-prey interactions with adaptive avoidance of predators, Bulletin of Mathematical Biology, 2017, vol. 79, no. 6, pp. 1325-1359, 2017.

[3] K. Kundu, S. Pal and S. Samanta, "Impact of fear effect in a discrete-time predator-prey system, " *Bull. Calcuta Math. Soc,* vol. 110, no.3, pp. 245-264, 2019.

[4] S. K. Sasmal, "Population dynamics with multiple Allee effects induced by fear factors-A mathematical study on prey-predator interactions,"*Applied Mathematical Modelling,* vol. 64, no.1, pp. 1-14, 2018.

[5] K. Fang, Z. Zhu, F. Chen, et al. "Qualitative and bifurcation analysis in a Leslie-Gower model with Allee effect," *Qualitative Theory of Dynamical Systems,* vol. 21, no.3, Article ID 86, 2022.

[6] X. Lin, X. Xie, et al, "Convergences of a stage-structured predator-prey model with modified Leslie-Gower and Holling-type II schemes," *Advances in Difference Equations,* 2016, 2016, Article ID 181.

[7] Z. Xiao, Z. Li, Z. Zhu, et al. "Hopf bifurcation and stability in a Beddington-DeAngelis predator-prey model with stage structure for predator and time delay incorporating prey refuge," *Open Mathematics,* vol. 17, no.1, pp. 141-159, 2019.

[8] Q. Yue, "Permanence of a delayed biological system with stage structure and density-dependent juvenile birth rate," *Engineering Letters,* vol. 27. no.2, pp. 263-268, 2019.

[9] X. Xie, Y. Xue, et al. "Permanence and global attractivity of a nonautonomous modified Leslie-Gower predator-prey model with Holling-type II schemes and a prey refuge,"*Advances in Difference Equations,* 2016, 2016, Article ID 184.

[10] H. Deng, F. Chen, Z. Zhu, et al, "Dynamic behaviors of Lotka-Volterra predator-prey model incorporating predator cannibalism,"*Advances in Difference Equations,* 2019, Article ID 359.

[11] F. D. Chen, Q. X. Lin, X. D. Xie, et al, "Dynamic behaviors of a nonautonomous modified Leslie-Gower predator-prey model with Holling-type III schemes and a prey refuge," *Journal of Mathematics and Computer Science,* vol.17, no.2, pp. 266-277, 2017.

[12] F. Chen, X. Guan, X. Huang, et al. "Dynamic behaviors of a Lotka-Volterra type predator-prey system with Allee effect on the predator species and density dependent birth rate on the prey species," *Open Mathematics,* vol.17, no.1, pp.1186-1202, 2019.

[13] Z. W. Xiao, Z. Li, "Stability analysis of a mutual interference predator-prey model with the fear effect," *Journal of Applied Science and Engineering,* vol. 22, no.2, pp. 205-211, 2019.

[14] W. Yin, Z. Li, F. Chen, et al. "Modeling Allee effect in the Leslie-Gower predator-prey system incorporating a prey refuge," *International Journal of Bifurcation and Chaos,* vol.32, no.06, Article ID 2250086, 2022.

[15] Z. Zhu, Y. Chen, Z. Li, et al. "Stability and bifurcation in a Leslie-Gower predator-prey model with Allee effect," *International Journal of Bifurcation and Chaos,* vol.32, no.03, Article ID: 2250040, 2022.

[16] E. Klimczuk, L. Halupka, B. Czyz, et al. "Factors driving variation in biparental incubation behaviour in the reed warbler Acrocephalus scirpaceus, " *Ardea*, vol.103, no.1, pp.51-59, 2015.

[17] S. Jawad, D. Sultan, M. Winter, "The dynamics of a modified Holling-Tanner prey-predator model with wind effect, " *International Journal of Nonlinear Analysis and Applications*, vol. 12(Special Issue): pp. 2203-2210, 2021.

[18] C. Huang, F. Chen, Q. Zhu, et al. "How the wind changes the Leslie-Gower predator-prey system?," *IAENG International Journal of Applied Mathematics*, vol. 53, no.3, pp. 907-915, 2023.

[19] M. J. Cherry, B. T. Barton, "Effects of wind on predator-prey interactions, " *Food Webs,* vol.13, no.1, pp. 92-97, 2017.

[20] D. Barman, V. Kumar, J. Roy, et al. "Modeling wind effect and herd behavior in a predator-prey system with spatiotemporal dynamics, " *The European Physical Journal Plus*, vol.137, no.8, 950-960, 2022.

[21] D. Barman, J. Roy, S. Alam, "Impact of wind in the dynamics of prey-predator interactions," *Mathematics and Computers in Simulation*, vol.191, no.1, pp. 49-81, 2022.

[22] P. Panja, "Impacts of wind and anti-predator behaviour on predator-prey dynamics: a modelling study," *International Journal of Computing Science and Mathematics*, vol.15, no.4, pp. 396-407, 2022.

[23] M. A. Aziz-Alaoui, M. Daher Okiye, "Boundedness and global stability for a predator-prey model with modified Leslie-Gower and Holling-type II schemes." *Applied Mathematics Letters,* vol. 16, no.7, pp.1069-1075, 2003.

[24] A. Korobeinikov, "A Lyapunov function for Leslie-Gower predator-prey models," *Applied Mathematics Letters*, vol.14, no.3, pp. 697-699, 2001.

[25] F. Chen, Z. Li, Y. Huang. "Note on the permanence of a competitive system with infinite delay and feedback controls, " *Nonlinear Analysis: Real World Applications*, vol.8, no.2, pp. 680-687, 2007.

[26] Y. C. Zhou, Z. Jin, J. L. Qin, Ordinary Differential Equation and Its Ap- plication, Beijing, Science Press, 2003.

[27] T. C. Gard and T. G. Hallam, "Persistence in food webs-I Lotka-Volterra food chains," *Bull. Math. Biol.* vol.41, no.6, pp. 877-891, 1979.

[28] K. Fang, J. Chen, Z. Zhu, et al. "Qualitative and bifurcation analysis of a single species Logistic model with Allee effect and feedback control," *IAENG International Journal of Applied Mathematics*, vol. 52, no.2, pp320-326, 2022.

[29] F. Chen, S. Lin, S. Chen, et al. "Global stability of Leslie-Gower predator-prey model with density dependent birth rRate on prey species and prey refuge, " *WSEAS Transactions on Systems and Control*, vol.22, no.1, pp 41-48, 2023.

[30] Z. Zhu, F. Chen, L. Lai, et al. "Dynamic behaviors of a discrete May type cooperative system incorporating Michaelis-Menten type harvesting, " *IAENG International Journal of Applied Mathematics*, vol. 50, no.3, pp 458-467, 2020.

[31] X. R. Li, Q. Yue, F. D. Chen, "The dynamic behaviors of nonselective harvesting Lotka-Volterra predator-prey system with partial closure for populations and the fear effect of the prey species," *IAENG International Journal of Applied Mathematics*, vol. 53, no.3, pp818-825, 2023.

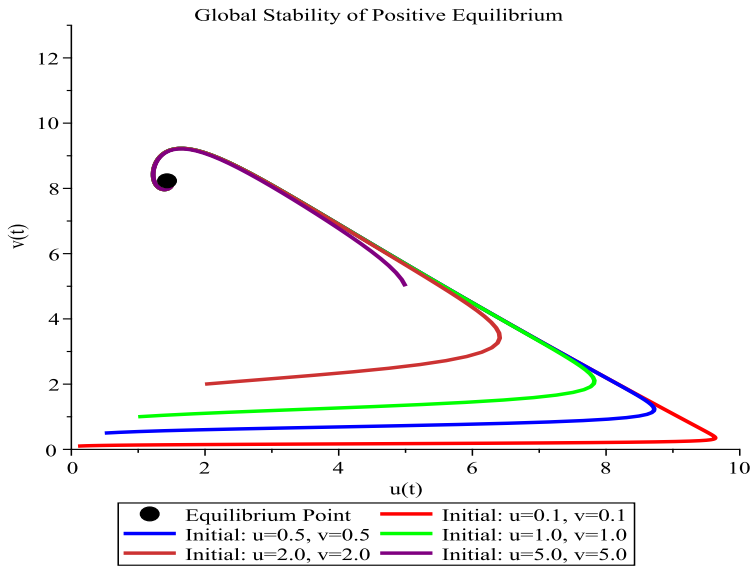

Fig. 1. Dynamic behaviors of the system (32), the initial condition $(u(0), v(0)) = (0.1, 0.1), (1, 1), (2, 2), (0.5, 0.5)$ and $(5, 5)$, respectively.

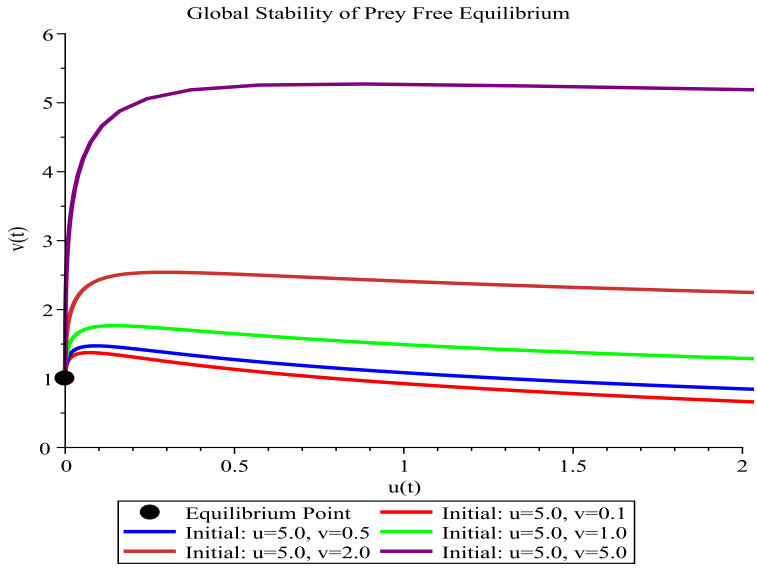

Fig. 2. Dynamic behaviors of the system (34), the initial condition $(u(0), v(0)) = (5, 0.1), (5, 0.5), (5, 1), (5, 2)$ and $(5, 5)$, respectively.

.

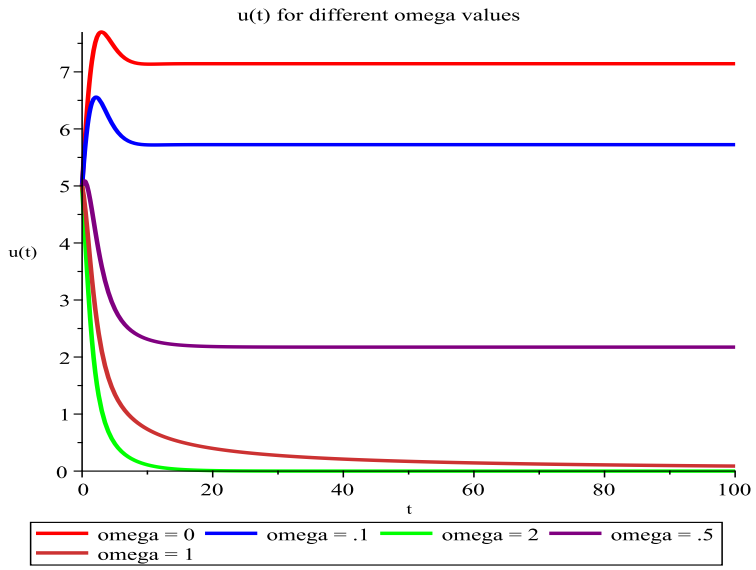

Fig. 3. The time series solution $u(t)$ corresponding to different ω values in system (35), where $\omega = 0, 0.1, 0.5, 1, 2$ and $(u(0), v(0)) = (20, 30)$. respectively.

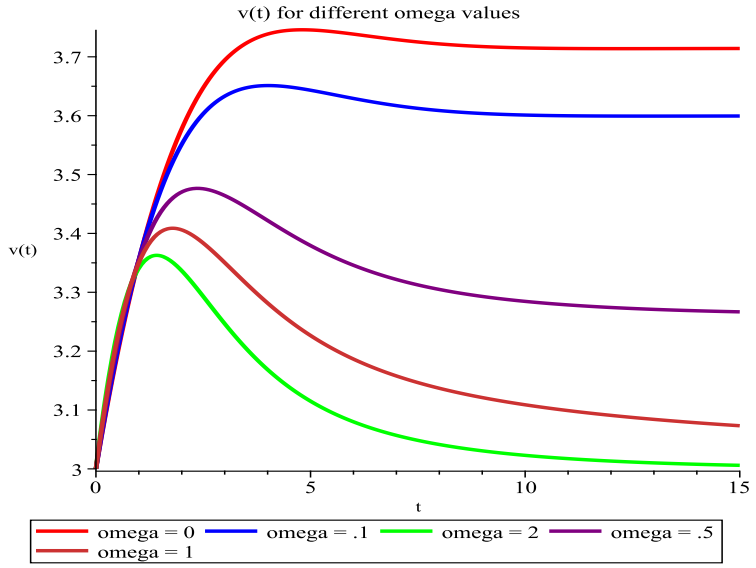

Fig. 4. The time series solution $v(t)$ corresponding to different ω values in system (35), where $\omega = 0, 1, 2, 3, 4$ and $(u(0), v(0)) = (20, 30)$. respectively.

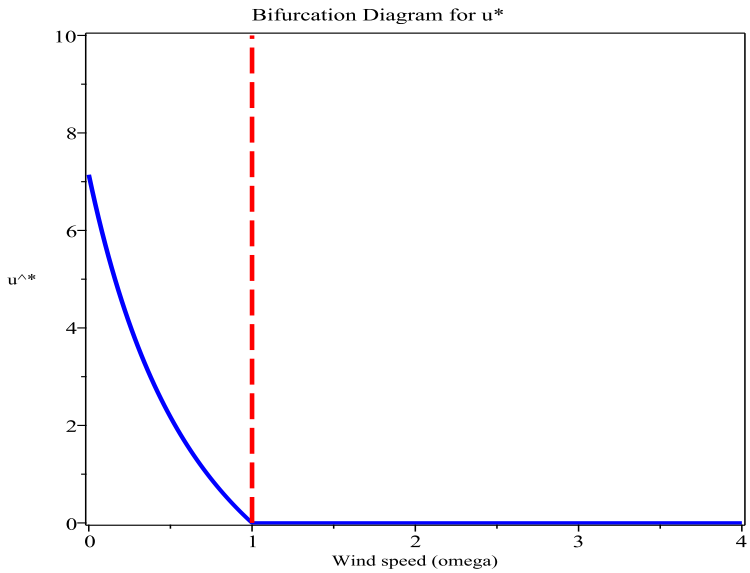

Fig. 5. Bifurcation Diagram of $u^*(\omega)$.

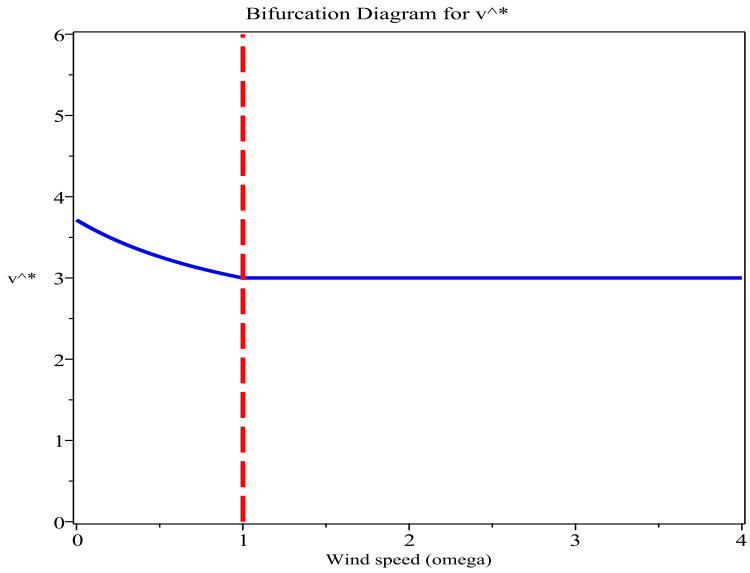

Fig. 6. Bifurcation Diagram of $v^*(\omega)$.

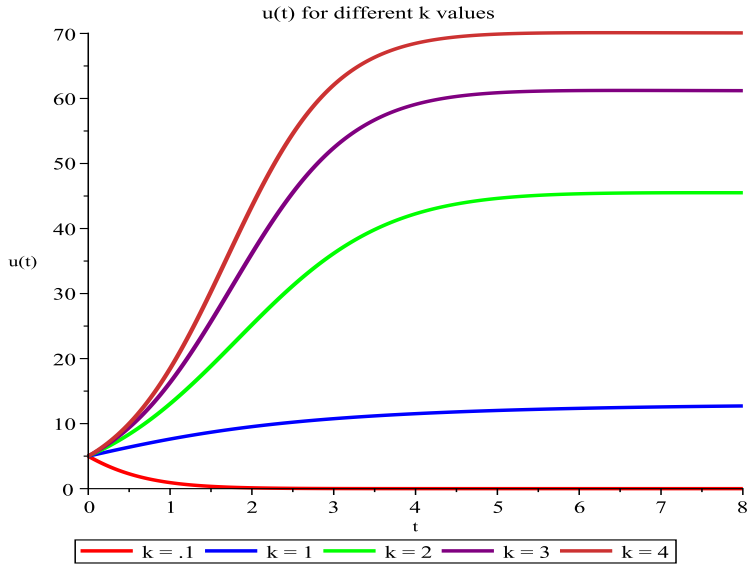

Fig. 7. Bifurcation Diagram of $u^*(k)$.

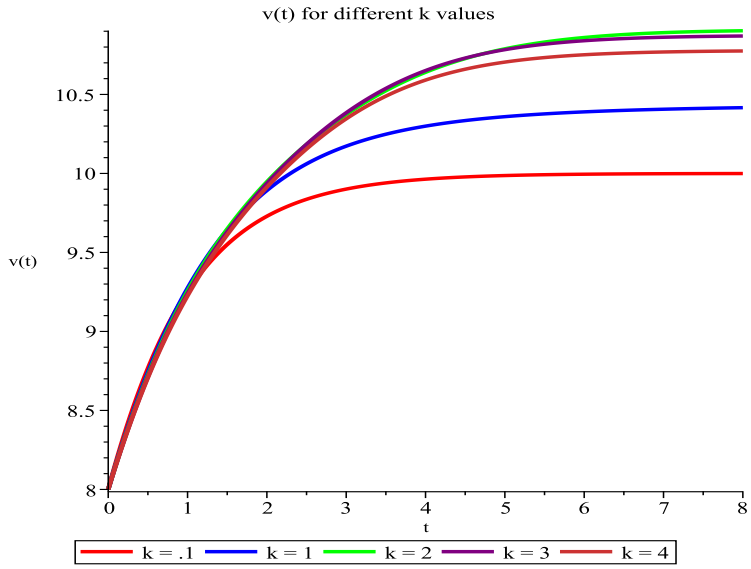

Fig. 8. Bifurcation Diagram of $v^*(k)$.

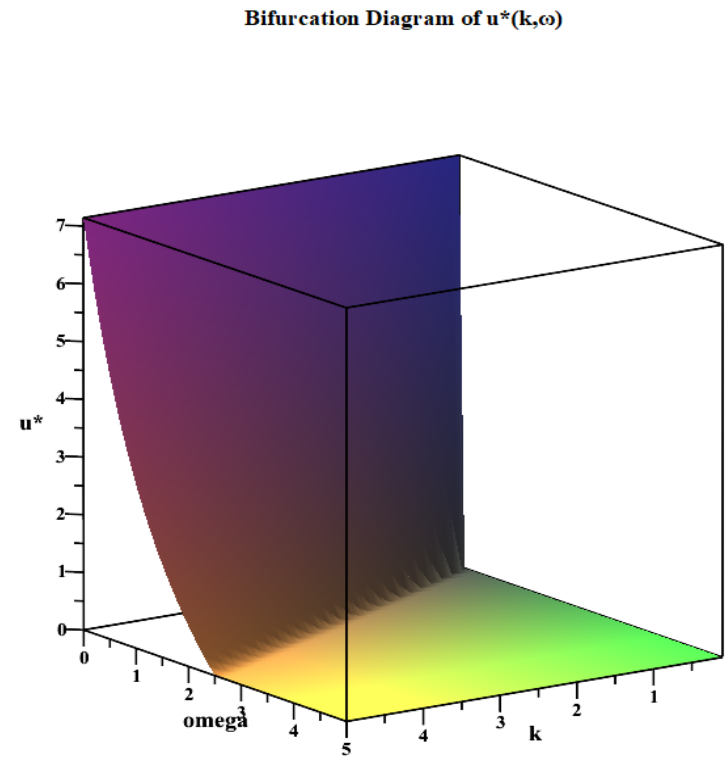

Fig. 9. Bifurcation Diagram of $u^*(k, \omega)$.

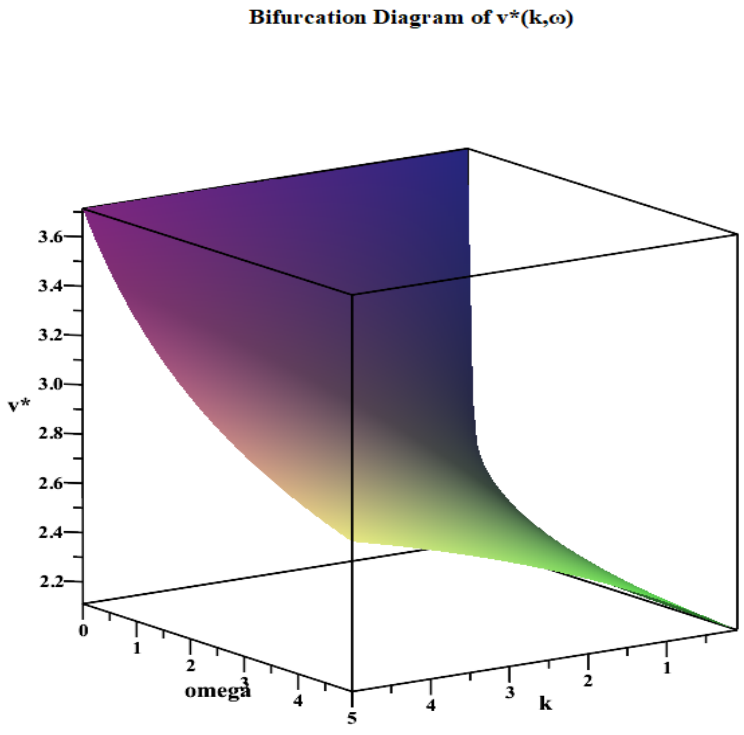

Fig. 10. Bifurcation Diagram of $v^*(k, \omega)$.

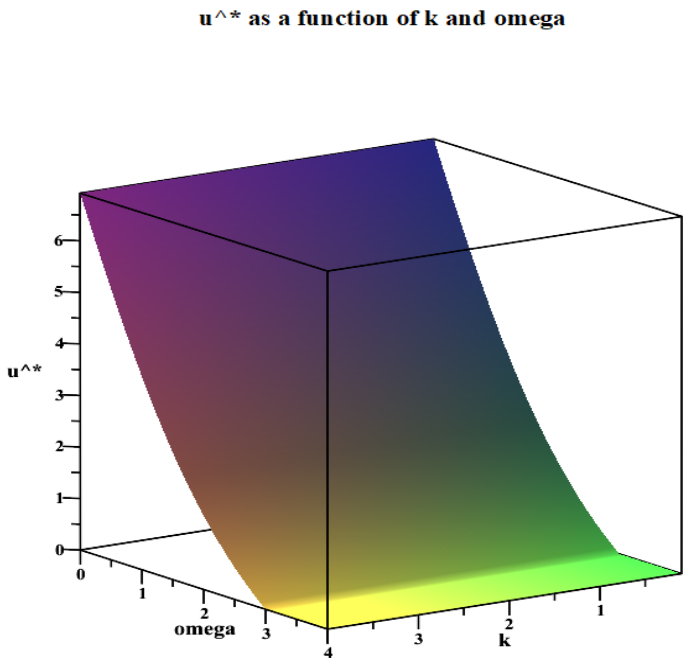

Fig. 11. Bifurcation Diagram of $u^*(\omega)$ of Case (1) in Example 10.4.

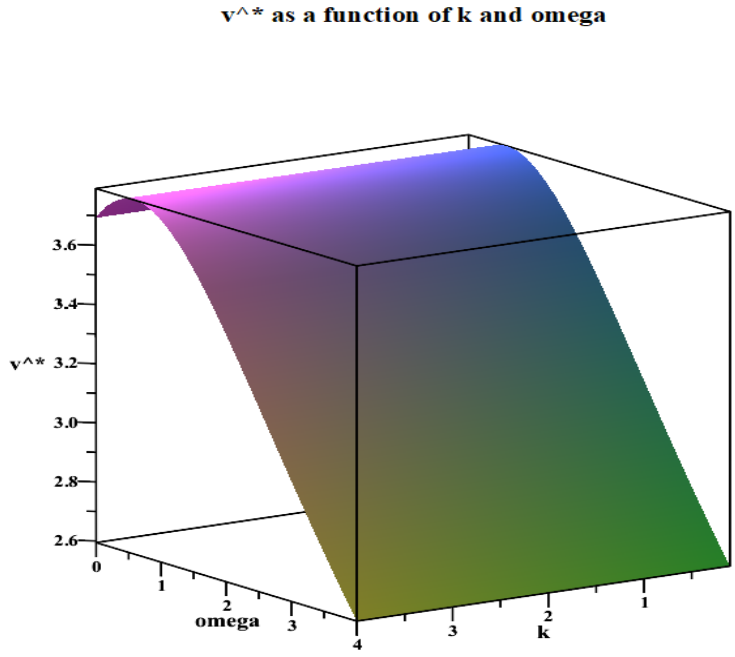

Fig. 12. Bifurcation Diagram of $v^*(\omega)$ of Case (1) in Example 10.4.

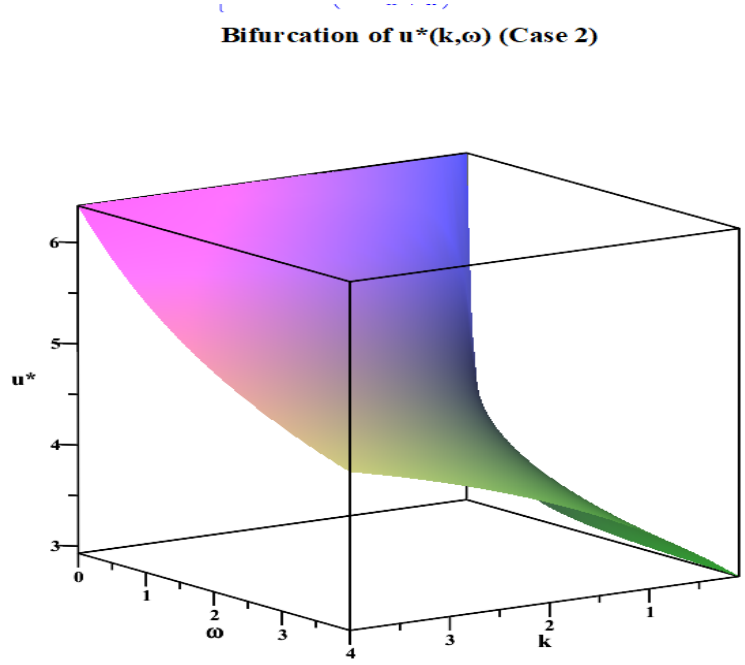

Fig. 13. Bifurcation Diagram of $u^*(k,\omega)$ of Case (2) in Example 10.4.

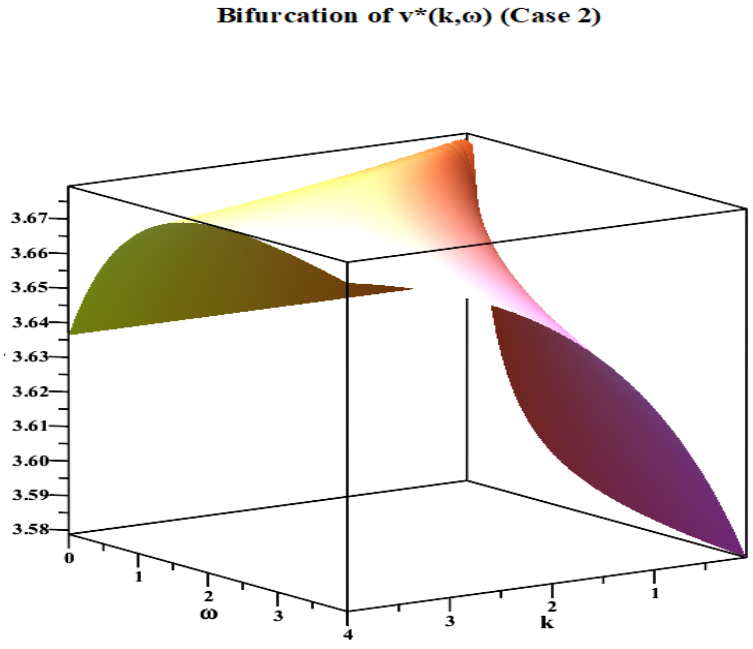

Fig. 14. Bifurcation Diagram of $v^*(k,\omega)$ of Case (2) in Example 10.4.